Supplemental Materials and Methods

Patient materials and T-Cell lines

One hundred and nineteen PTCL cases were included in the study (35 AITL, 69 PTCL-NOS, and 15 PTCL-T_{FH}). Twenty-nine were formalin fixed paraffin embedded (FFPE)[1], with the remaining samples being fresh frozen (FF). PTCL specimens were collected from the Nebraska Lymphoma Study Group (NLSG) registry and Tissue Bank, the International Peripheral T-cell Lymphoma (IPTCL) Consortium, or from generous collaborations. Twenty-five of the PTCL-NOS cases from a previous study[2] had corresponding CGH data and GEP data that allowed for GATA3/TBX21 subgroup classification. For three PTCL-NOS cases, CNAs were obtained from next generation sequencing (NGS) data[3] and included in **Figure-6**. The clinical and pathological characteristics are tabulated in **Table-S1**. **Table-S1** shows detailed information regarding sample description, aCGH platform, molecular classification, ABSOLUTE (V1.0.06) purity, and immunohistochemistry (IHC) data. One hundred and five of the cases were included in previous profiling studies[1,2,4,5] and were reviewed by at least two pathologists to reach a consensus diagnosis. Additional PTCL series were included for comparative analysis[6-10]. This study was approved by the Institutional Review Board of the University of Nebraska Medical Center.

Four T-cell lines representative of lymphoblastic leukemia (Jurkat), Sezary Syndrome (HuT78), CTCL/ALCL ALK- (MAC-1[11,12]), and a mature $CD4^{-}CD8^{+}$ T-cell lymphoma (T8ML1[13]) were used in the study. These T-cell lines were cultured in 2.05mM L-Glutamine supplemental RPMI 1640 (HyClone) (T8ML1, MAC-1, Jurkat) or IMDM (HuT78), supplemented with 10% or 20% fetal bovine serum (FBS) respectively, penicillin G (199 U/ml) and streptomycin (100 µg/ml). T8ML1 was further supplemented with IL-2 (10 ng/ml). Cell cultures were maintained at 37ºC in 5% CO_2. All cell lines underwent routine mycoplasma testing using the Universal Mycoplasma Detection Kit (ATCC), with the most recent testing completed on August 17, 2017. Approximately, four passages of the cells occurred between thawing and experimental use. The T8ML1 cell line was generously provided from Hiroshi Fujiwara, whom was involved in establishing the cell line[13]. MAC-1 was originally established by Marshall Kadin[14]. Both Jurkat and HuT78 were previously purchased from ATCC. The status of *PTEN* and *TP53* mutation and copy number are indicated in **Table-S2**.

Molecular classification of cases with FFPE-derived GEP and RNA-seq

Sixty-three cases had previously undergone molecular classification according to the gene signatures previously described[4,5]. The remaining cases were classified using the Affymetrix U133 Plus2 data, RNA-seq data, or Illumina DASL mRNA expression data and the same gene signatures and Bayesian algorithm described in the previous publications[4,5].

RNA-sequencing (RNA-seq) on an additional nine AITL cases classified by morphology and immunohistochemistry (IHC) was performed using RNA-TruSeq mRNA Library Preparation Kits (Illumina, San Diego, CA, USA) and an Illumina HiSeq 2000 sequencer. Tophat, Cufflinks, and Cuffdiff[15] were used for alignment, read counting, and generation of FPKM values. We used a pre-defined AITL mRNA signature derived from a well-characterized histopathological AITL training cohort from earlier studies[4,5] and using the

Bayesian algorithm validated eight (of nine) new AITL cases having a high probability (>0.80) with the AITL signature and thus were included in this study.

The Affymetrix HG-U133 Plus2 data from PTCL-GATA3 and PTCL-TBX21 cases from a previous study[5] was imported into BRB array tools (https://brb.nci.nih.gov/BRB-ArrayTools/) and MAS5.0 normalized, as previously described[5]. Data on the Illumina DASL platform from a previous study[1] was separately imported and normalized using BRB ArrayTools. The normalized data from each array platform was exported and the maximally expressed probe set was selected for each gene. The data from the two platforms were merged and the two platforms were cross-platform normalized using the empirical Bayes method (ComBat)[16]. For individual arrays, the correlation between probe set values before and after combat was approximately 0.8-0.98. We re-examined each transcript that was included in the original signature[5] and present in both platforms and selected the transcripts that expressed a positive correlation with the classifier's mean in the FFPE data. The classifier genes were then used for Bayesian classification in FFPE cases, with the HG-U133 Plus2 cases of known classification serving as a training set, as performed in previous studies[4,5]. The cases were classified, if it showed >80% probability of belonging to one subgroup versus other groups as shown in previous studies[4,5]. Additionally, we also performed unsupervised hierarchical clustering using the classifier genes in the cases included in the CNA study and confirmed that there were two main clusters, one dominated by PTCL-GATA3 cases and one dominated by PTCL-TBX21 cases (data not shown), indicating the magnitude of the differential expression of the classifier genes can tolerate the platform differences.

DNA copy number analysis

Genomic DNA was previously extracted from FF tissues using the AllPrep DNA/RNA kit (Qiagen) and from FFPE samples using AllPrep DNA/RNA FFPE kit (Qiagen). Three different SNP array platforms (Nsp1 SNP 250K, SNP 6.0 and OncoScan, Affymetrix) were used for copy number (CN) analysis together with previously publish Agilent SurePrint aCGH data[2]. DNA libraries were generated according to the manufacturer's recommendations specific to each platform. Specifically for the OncoScan platform, two raw .CEL files are generated, one for the "AT" array and a second for the "GC" array. The .CEL files are combined in OncoScan Console (Affymetrix) to generate a single .OSCHP file. Briefly, the generation of the .OSCHP file entails calculating the log2 ratio, allelic difference and B-allele frequency (BAF), then identifying normal diploid regions. Based on the normal diploid regions, the log2 ratio, allelic difference, and BAF are recomputed if necessary. Visualization of the copy number abnormalities (CNAs) was performed with Nexus Copy Number™ software (Bio Discovery, El Segundo, CA, USA) which enables multiple platform analysis using the SNP-FASST2 algorithm. For cases with paired normal (11 AITL on SNP 6.0), Nexus Copy Number enables the combined import of tumor and normal sample. The gain and loss thresholds were set at a log2 ratio of 0.06 and -0.06, respectively. Raw data from deposited CEL files from published studies[8,10] were analyzed using the SNP-FASST2 algorithm with default settings. Segmentation files for the published ALCL study[6] were observed. The percent aberrant genome per case was calculated by taking the total size of the aberrant regions divided by the total size of the genome for chromosomes 1-22. Frequencies of gains and losses along the

chromosomes were calculated by Nexus and moving average smoothing at 5 Mb was applied for CNA frequency along the chromosome plots.

Integrative analysis of CNAs with GEP

Total RNA isolated from FF and FFPE PTCL cases was previously used to obtain GEP data (Affymetrix HG-U133 Plus2 and Illumina DASL) and was included in previous studies[1,2,4,5]. For each gene the probeset with the maximal expression was used. For cases with GEP data on the Affymetrix HG-U133 Plus2, we compared the average mRNA expression level of genes against CN status (gain/amplification, heterozygous/homozygous loss, 2N) using one-sided Student's t-test to determine significance. Ingenuity pathway analysis (IPA) program (Qiagen, Inc) or DAVID v6.8 (https://david.ncifcrf.gov/) was used for the molecular and functional annotation of the genes within aberrant regions, and only pathways with $p<0.05$ and an FDR<0.25 were included in the discussion.

Unsupervised hierarchical clustering

Unsupervised hierarchical clustering of molecularly classified PTCL-NOS cases was performed using the CN status of abnormalities identified at a frequency $\geq$10% in either the PTCL-GATA3 or PTCL-TBX21 subgroups. An arm was considered lost or gained accordingly if at least 25% of the arm displayed the aberration. Clustering was performed using Cluster 3.0 (correlation (centered)) similarity metric and average linkage, http://bonsai.hgc.jp/~mdehoon/software/cluster/software.htm). The two validation cohorts were clustered similarly based on the abnormalities identified in the molecularly classified/training series. Correlation of CNAs among cases was performed using Pearson correlation and the R-language "corrplot" package.

NanoString nCounter v2 Cancer CN Assay

The v2 Cancer CN Assay provides analysis of 87 genes commonly found aberrant in cancer and has been optimized for the use of FFPE samples as well. Fifty-four probes targeting invariant regions are also included as controls. DNA (500 ng) was fragmented with AluI restriction enzyme followed by a 24 hour hybridization per the manufacturer. Post-hybridization purification was performed by the nCounter Prep Station followed by image acquirement at maximum sensitivity on the nCounter Digital Analyzer. Subsequent analysis was completed using nSolver Analysis Software 3.0 as suggested per the manufacturer.

Genomic sequencing and analysis

A custom panel targeting 334 genes recurrently mutated in non-Hodgkin lymphomas (NHLs) was previously designed using the Agilent SureSelect platform. Fifteen-18 samples were sequenced per lane on an Illumina HiSeq2500 sequencer for an average of 268-fold coverage of targeted regions. Adapter sequences were trimmed using trimmomatic (v0.36). Raw reads were mapped to the human genome (hg19) using the Burrows-Wheeler Aligner-MEM (v0.7.15). Genome Analysis Toolkit (v3.6) was used for local realignment and base quality recalibration. Duplicate marking was done with Picard (v2.4.1). Variant calling and filtering were performed with VarScan 2 (v2.4.0) and Genome Analysis Toolkit UnifiedGenotyper. The variants were

annotated using Annovar (http://annovar.openbioinformatics.org). Variant filters applied included requiring that variants should be supported by at least four reads with a minimal variant allelic frequency of 5% with variant reads on the plus and minus strand. Variants were excluded if they 1) existed in the dbSNP138NotFlagged database (http://annovar.openbioinformatics.org/en/latest/user-guide/filter); 2) were in a regions of segmental duplication (SuperDups, Annovar); 3) did not change protein sequences or affect splice sites; 4) were recurrent in a set of 92 unrelated normal samples; or 5) were shared by >10 cases unless they are from a gene known to have frequent mutations and thus present in the COSMIC database.

Overall survival outcome analysis

The overall survival (OS; death from any cause) was estimated using the Kaplan-Meier method, and differences assessed using the log-rank test. Statistical analyses were performed with the R-language survival package. Differences among groups were considered significant at p-values below 0.05 (*).

PrestoBlue assay

Jurkat, T8ML1, MAC-1, and HuT78 cell lines were treated with different concentrations of Torin 1 (10189-392, BioVision) (100, 200 and 300 nM), Torin 2 (2274-5, BioVision) (10, 20, 40, 60 and 100 nM), and Temsirolimus (TEM) (Chemscene) (1, 2, 3, 4, and 5 µM) for 24 hours. Sensitivity to drug treatment in the four cell lines was assayed in 96 well plates using PrestoBlue™ Cell Viability Reagent (Invitrogen -A13261) per manufacture's protocol and read on a Tecan Infinite M200Pro.

Western blotting

Jurkat, T8ML1, MAC-1, and HuT78 cell lines were treated with Torin 1 (200 nM), Torin 2 (100 nM), or TEM (2 µM) for 24 hours and then lysed in RIPA buffer (50 mM Tris, pH 7.4, 150 mM NaCl,1% Triton X-100, 0.1% SDS, 1% sodium deoxycholate, 10 mM sodium 2-glycerolphosphate, 1 mM phenylmethylsulfonyl fluoride, 0.4 units/ml aprotinin, 1 mM sodium fluoride, and 0.1 mM sodium vanadate). Twenty to 100 µG of whole-cell extracts were separated by sodium dodecyl sulfate-polyacrylamide gel electrophoresis and transferred to nitrocellulose (Bio-Rad) or polyvinylidene difluoride (Bio-Rad) membranes. Membranes were blocked in Odyssey Blocking Buffer (LI-COR) or Tris buffered saline with 0.1% Tween and 5% milk at room temperature for 30 minutes to 1 hour and then incubated with primary antibody specific to pAKT (S473) (#4060;CST), pAKT (Thr308) (#13038;CST), total AKT (#4691;CST), p4EBP1 (#2855;CST), p-RPS6 (#4858;CST), caspase-3 (#9661;CST), and β-actin (#1616;SC) at 4°C overnight, followed by treatment with secondary antibodies.

Genomic status of *PTEN* and *TP53*

The genomic DNA from T-cell lines was used to quantify the DNA copy number of *PTEN* and *TP53* in comparison to *RPL13A*, and tonsillar DNA was used as a calibrator (normal). Two Burkitt Lymphoma (BL) cell lines (Raji and Namalwa) were included as positive controls. The qPCR experiment was performed using SYBR Green qPCR Kit (Bio Rad. Inc) using primers listed in **Table-S2**. The standard ΔΔ CT (CT (*PTEN* or *TP53*)–CT (*RPL13A*) method was used to estimate the status of the genomic locus.

References

1. Piccaluga PP, Fuligni F, De Leo A, Bertuzzi C, Rossi M, Bacci F, et al. Molecular profiling improves classification and prognostication of nodal peripheral T-cell lymphomas: results of a phase III diagnostic accuracy study. *J Clin Oncol.* 2013;31(24):3019-3025.
2. Dobay MP, Lemonnier F, Missiaglia E, Bastard C, Vallois D, Jais JP, et al. Integrative clinicopathological and molecular analyses of angioimmunoblastic T-cell lymphoma and other nodal lymphomas of follicular helper T-cell origin. *Haematologica.* 2017;102(4):e148-e151.
3. Kuilman T, Velds A, Kemper K, Ranzani M, Bombardelli L, Hoogstraat M, et al. CopywriteR: DNA copy number detection from off-target sequence data. *Genome Biol.* 2015;16:49.
4. Iqbal J, Weisenburger DD, Greiner TC, Vose JM, McKeithan T, Kucuk C, et al. Molecular signatures to improve diagnosis in peripheral T-cell lymphoma and prognostication in angioimmunoblastic T-cell lymphoma. *Blood.* 2010;115(5):1026-1036.
5. Iqbal J, Wright G, Wang C, Rosenwald A, Gascoyne RD, Weisenburger DD, et al. Gene expression signatures delineate biological and prognostic subgroups in peripheral T-cell lymphoma. *Blood.* 2014;123(19):2915-2923.
6. Boi M, Rinaldi A, Kwee I, Bonetti P, Todaro M, Tabbo F, et al. PRDM1/BLIMP1 is commonly inactivated in anaplastic large T-cell lymphoma. *Blood.* 2013;122(15):2683-2693.
7. Hartmann S, Gesk S, Scholtysik R, Kreuz M, Bug S, Vater I, et al. High resolution SNP array genomic profiling of peripheral T cell lymphomas, not otherwise specified, identifies a subgroup with chromosomal aberrations affecting the REL locus. *British journal of haematology.* 2010;148(3):402-412.
8. Lin WM, Lewis JM, Filler RB, Modi BG, Carlson KR, Reddy S, et al. Characterization of the DNA copy-number genome in the blood of cutaneous T-cell lymphoma patients. *The Journal of investigative dermatology.* 2012;132(1):188-197.
9. Nakagawa M, Nakagawa-Oshiro A, Karnan S, Tagawa H, Utsunomiya A, Nakamura S, et al. Array comparative genomic hybridization analysis of PTCL-U reveals a distinct subgroup with genetic alterations similar to lymphoma-type adult T-cell leukemia/lymphoma. *Clin Cancer Res.* 2009;15(1):30-38.
10. Yamagishi M, Nakano K, Miyake A, Yamochi T, Kagami Y, Tsutsumi A, et al. Polycomb-mediated loss of miR-31 activates NIK-dependent NF-kappaB pathway in adult T cell leukemia and other cancers. *Cancer cell.* 2012;21(1):121-135.
11. Ehrentraut S, Schneider B, Nagel S, Pommerenke C, Quentmeier H, Geffers R, et al. Th17 cytokine differentiation and loss of plasticity after SOCS1 inactivation in a cutaneous T-cell lymphoma. *Oncotarget.* 2016;7(23):34201-34216.
12. Piva R, Pellegrino E, Mattioli M, Agnelli L, Lombardi L, Boccalatte F, et al. Functional validation of the anaplastic lymphoma kinase signature identifies CEBPB and BCL2A1 as critical target genes. *The Journal of clinical investigation.* 2006;116(12):3171-3182.
13. An J, Fujiwara H, Suemori K, Niiya T, Azuma T, Tanimoto K, et al. Activation of T-cell receptor signaling in peripheral T-cell lymphoma cells plays an important role in the development of lymphoma-associated hemophagocytosis. *International journal of hematology.* 2011;93(2):176-185.
14. Kadin ME, Cavaille-Coll MW, Gertz R, Massague J, Cheifetz S, George D. Loss of receptors for transforming growth factor beta in human T-cell malignancies. *Proc Natl Acad Sci U S A.* 1994;91(13):6002-6006.
15. Trapnell C, Roberts A, Goff L, Pertea G, Kim D, Kelley DR, et al. Differential gene and transcript expression analysis of RNA-seq experiments with TopHat and Cufflinks. *Nat Protoc.* 2012;7(3):562-578.
16. Johnson WE, Li C, Rabinovic A. Adjusting batch effects in microarray expression data using empirical Bayes methods. *Biostatistics.* 2007;8(1):118-127.

Table-S1: Case IDs and corresponding data. Cases indicated with "*" in the first column were sequenced.

Case	Classification	CN Platform	Previously Published CN Data	GEP Platform	GEO Deposited GEP	Previously Published GEP	CN Tissue Source	% Large Neoplastic T-cell	Absolute Purity	CD3	CD4	CD8	CD30	CD10	PD1	CXCL13	ICOS	CCR5	SAP	BCL6
AITL1	AITL	OncoScan	No	HG-U133 Plus2	GSM472085	Yes[2]	Fresh Frozen	22.5	24.00%	+	+	-		+						
AITL2	AITL	OncoScan	No	HG-U133 Plus2	GSM472137	Yes[2]	Fresh Frozen	45	24.00%	+	+	-	-	-						
AITL3	AITL	OncoScan	No	HG-U133 Plus2	GSM1411444	Yes[3]	Fresh Frozen		22.00%	+	+	-		Partial		+				+
AITL4	AITL	OncoScan	No	HG-U133 Plus2	GSM1411340	Yes[3]	Fresh Frozen		18.00%											
AITL5	AITL	OncoScan	No	HG-U133 Plus2	GSM472142	Yes[2]	Fresh Frozen	62.5	23.00%	+	+	-	+							
AITL6	AITL	OncoScan	No	HG-U133 Plus2	GSM1411347	Yes[3]	Fresh Frozen		21.00%	+	+	-	-							
AITL7	AITL	OncoScan	No	HG-U133 Plus2	GSM1411304	Yes[3]	Fresh Frozen		19.00%	+	+	-	Weak	Weak	Weak					
AITL8	AITL	OncoScan	No	HG-U133 Plus2	GSM1411296	Yes[3]	Fresh Frozen		31.00%	+	+	-	-	Weak	Weak	+				-
AITL9	AITL	OncoScan	No	HG-U133 Plus2	GSM1411443	Yes[3]	Fresh Frozen		18.00%	+	+	-	-	Partial						
AITL10	AITL	OncoScan	No	HG-U133 Plus2	GSM1411462	Yes[3]	Fresh Frozen		15.00%	+	+	-	-	-	+					
AITL11	AITL	OncoScan	No	HG-U133 Plus2	GSM1411344	Yes[3]	Fresh Frozen		18.00%	+										
AITL12	AITL	OncoScan	No	HG-U133 Plus2	Pending GEO Deposit	No	Fresh Frozen	80	18.00%	-										
AITL13	AITL	OncoScan	No	HG-U133 Plus2	GSM1411365	Yes[3]	Fresh Frozen	70	25.00%	+	+	-								
AITL14	AITL	OncoScan	No	HG-U133 Plus2	Pending GEO Deposit	No	Fresh Frozen		22.00%	+	-	-	+	+						
AITL15	AITL	OncoScan	No	HG-U133 Plus2	GSM1411308	Yes[3]	Fresh Frozen		21.00%	+	+	-	-	-	Weak					
AITL16	AITL	OncoScan	No	HG-U133 Plus2	GSM1411362	Yes[3]	Fresh Frozen		43.00%	+	+	-		+						
AITL17	AITL	OncoScan	No	HG-U133 Plus2	GSM1411300	Yes[3]	Fresh Frozen		17.00%	+	+	-	Weak		+					
AITL18	AITL	OncoScan	No	HG-U133 Plus2	GSM1411303	Yes[3]	Fresh Frozen		18.00%	+	+	-	Weak		+					
AITL19	AITL	OncoScan	No	HG-U133 Plus2	GSM1411305	Yes[3]	Fresh Frozen		23.00%	+	+	-	-		+					
AITL20	AITL	OncoScan	No	HG-U133 Plus2	GSM1411463	Yes[3]	Fresh Frozen		20.00%	+	+	-	-							
AITL21	AITL	SNP 250K	No	HG-U133 Plus2	Pending GEO Deposit	No	Fresh Frozen	50	30.00%	+	+	-	-	-						
AITL22	AITL	SNP 250K	No	HG-U133 Plus2	GSM472083	Yes[2]	Fresh Frozen	40	28.00%	+	|	-		-						
AITL23	AITL	SNP 250K	No	HG-U133 Plus2	Pending GEO Deposit	No	Fresh Frozen	40	25.00%	+	+	-		+						
AITL24	AITL	SNP 250K	No	HG-U133 Plus2	GSM472086	Yes[2]	Fresh Frozen	32.5	38.00%	+	|	-		+						
AITL25	AITL	SNP 250K	No	HG-U133 Plus2	GSM1411348	Yes[3]	Fresh Frozen		24.00%	+	+			+						
AITL26	AITL	SNP 250K	No	HG-U133 Plus2	GSM1411356	Yes[3]	Fresh Frozen	30	23.00%	+	+	-	|	+						
AITL27	AITL	SNP 250K	No	HG-U133 Plus2	GSM472062	Yes[2]	Fresh Frozen	50	35.00%	+	+	-								
AITL28	AITL	SNP 6.0	No	RNA-Sequencing Illumina	Pending Deposit	No	Fresh Frozen	80	18.00%	+	+	-	-	+	+					+
AITL29	AITL	SNP 6.0	No	RNA-Sequencing Illumina	Pending Deposit	No	Fresh Frozen	80	50.00%	+	+	-		-	+					+
AITL30	AITL	SNP 6.0	No	RNA-Sequencing Illumina	Pending Deposit	No	Fresh Frozen	80	27.00%	+	+	-	+ Scattered	-	+					+
AITL31	AITL	SNP 6.0	No	RNA-Sequencing Illumina	Pending Deposit	No	Fresh Frozen		27.00%	+	+	+		+	+					
AITL32	AITL	SNP 6.0	No	RNA-Sequencing Illumina	Pending Deposit	No	Fresh Frozen		18.00%	+/-	+	-		+	+					
AITL33	AITL	SNP 6.0	No	RNA-Sequencing Illumina	Pending Deposit	No	Fresh Frozen		66.00%	+	+	-/+		-/+	+					
AITL34	AITL	SNP 6.0	No	RNA-Sequencing Illumina	Pending Deposit	No	Fresh Frozen		21.00%	+				+/-	+					+
AITL35	AITL	SNP 6.0	No	RNA-Sequencing Illumina	Pending Deposit	No	Fresh Frozen	80	24.00%	+/-	+	-	-	+	+					
PTCL-NOS1*	PTCL-GATA3	OncoScan	No	DASL Illumina	PTCL_NOS_028	Yes[4]	FFPE		18.00%	+	+	+		-	-	-				-
PTCL-NOS2*	PTCL-GATA3	OncoScan	No	DASL Illumina	PTCL_NOS_039	Yes[4]	FFPE		16.00%	+	+	-/+	-/+	-	+	-				-
PTCL-NOS3*	PTCL-GATA3	OncoScan	No	DASL Illumina	PTCL_NOS_041	Yes[4]	FFPE		20.00%	+	-/+	-	-	-	+	-				-
PTCL-NOS4	PTCL-GATA3	OncoScan	No	DASL Illumina	PTCL_NOS_037	Yes[4]	FFPE		23.00%	+	+	-	-	-	+	-				-
PTCL-NOS5*	PTCL-GATA3	OncoScan	No	DASL Illumina	PTCL_NOS_034	Yes[4]	FFPE		26.00%	+	+	-	+/-	-	-	-				-
PTCL-NOS6*	PTCL-GATA3	OncoScan	No	DASL Illumina	PTCL_NOS_064	Yes[4]	FFPE		23.00%	+	-	+		-	Rare+	Rare+				Rare+
PTCL-NOS7*	PTCL-GATA3	OncoScan	No	DASL Illumina	PTCL_NOS_065	Yes[4]	FFPE		70.00%	+	+	-	-	-	-	-				-
PTCL-NOS8	PTCL-GATA3	Agilent SurePrint	Yes[1]	HG-U133 Plus2	Yes[1]	Yes[1]	Fresh Frozen		31.00%	Reviewed in Dobay et al, Haematologica 2017										
PTCL-NOS9	PTCL-GATA3	Agilent SurePrint	Yes[1]	HG-U133 Plus2	Yes[1]	Yes[1]	Fresh Frozen		42.00%	Reviewed in Dobay et al, Haematologica 2017										
PTCL-NOS10	PTCL-GATA3	Agilent SurePrint	Yes[1]	HG-U133 Plus2	Yes[1]	Yes[1]	Fresh Frozen		28.00%	Reviewed in Dobay et al, Haematologica 2017										
PTCL-NOS11	PTCL-GATA3	Agilent SurePrint	Yes[1]	HG-U133 Plus2	Yes[1]	Yes[1]	Fresh Frozen		27.00%	Reviewed in Dobay et al, Haematologica 2017										
PTCL-NOS12	PTCL-GATA3	Agilent SurePrint	Yes[1]	HG-U133 Plus2	Yes[1]	Yes[1]	Fresh Frozen		68.00%	Reviewed in Dobay et al, Haematologica 2017										
PTCL-NOS13	PTCL-GATA3	Agilent SurePrint	Yes[1]	HG-U133 Plus2	Yes[1]	Yes[1]	Fresh Frozen		29.00%	Reviewed in Dobay et al, Haematologica 2017										
PTCL-NOS14	PTCL-GATA3	Agilent SurePrint	Yes[1]	HG-U133 Plus2	Yes[1]	Yes[1]	Fresh Frozen		70.00%	Reviewed in Dobay et al, Haematologica 2017										
PTCL-NOS15	PTCL-GATA3	Agilent SurePrint	Yes[1]	HG-U133 Plus2	Yes[1]	Yes[1]	Fresh Frozen		29.00%	Reviewed in Dobay et al, Haematologica 2017										
PTCL-NOS16	PTCL-GATA3	Agilent SurePrint	Yes[1]	HG-U133 Plus2	Yes[1]	Yes[1]	Fresh Frozen		30.00%	Reviewed in Dobay et al, Haematologica 2017										
PTCL-NOS17*	PTCL-GATA3	Not Available	No	HG-U133 Plus2	GSM472059	Yes[2]	Fresh Frozen		Not Available											
PTCL-NOS18*	PTCL-GATA3	OncoScan	No	HG-U133 Plus2	GSM1411359	Yes[3]	Fresh Frozen	50	32.00%	+	+	-	-	-	-	-	-			
PTCL-NOS19	PTCL-GATA3	OncoScan	No	HG-U133 Plus2	GSM472055	Yes[2]	Fresh Frozen	30	42.00%	+	+	-								
PTCL-NOS20*	PTCL-GATA3	OncoScan	No	HG-U133 Plus2	GSM1411372	Yes[3]	Fresh Frozen	20	28.00%	+	|	-	-		-	-	-			
PTCL-NOS21*	PTCL-GATA3	OncoScan	No	HG-U133 Plus2	GSM472075	Yes[2]	Fresh Frozen	70	44.00%	+	+	-	-		-	-	-			
PTCL-NOS22*	PTCL-GATA3	OncoScan	No	HG-U133 Plus2	GSM1411455	Yes[3]	Fresh Frozen	60	35.00%	+	+	-	-	-	-	-	-			
PTCL-NOS23*	PTCL-GATA3	OncoScan	No	HG-U133 Plus2	GSM472156	Yes[2]	Fresh Frozen	41.25	46.00%	+	-	-	+							
PTCL-NOS24*	PTCL-GATA3	OncoScan	No	HG-U133 Plus2	GSM472073	Yes[2]	Fresh Frozen	20	23.00%	+	+	-	+							
PTCL-NOS25*	PTCL-GATA3	OncoScan	No	HG-U133 Plus2	GSM1411352	Yes[3]	Fresh Frozen	15	32.00%	-	+	-								
PTCL-NOS26	PTCL-GATA3	OncoScan	No	HG-U133 Plus2	GSM1411338	Yes[3]	Fresh Frozen		17.00%											
PTCL-NOS27	PTCL-GATA3	OncoScan	No	HG-U133 Plus2	GSM472071	Yes[2]	Fresh Frozen	60	32.00%	+	-	-			-	-	-			
PTCL-NOS28*	PTCL-GATA3	OncoScan	No	HG-U133 Plus2	GSM1411417	Yes[3]	FFPE	80	53.00%						-	-	+			
PTCL-NOS29*	PTCL-GATA3	OncoScan	No	HG-U133 Plus2	Pending GEO Deposit	No	Fresh Frozen		23.00%	+	+	-	-							
PTCL-NOS30	PTCL-GATA3	OncoScan	No	HG-U133 Plus2	GSM1411295	Yes[3]	FFPE	80	39.00%						-	-	+			
PTCL-NOS31	PTCL-GATA3	OncoScan	No	HG-U133 Plus2	GSM1411297	Yes[3]	Fresh Frozen		29.00%											
PTCL-NOS32*	PTCL-GATA3	OncoScan	No	HG-U133 Plus2	GSM1411428	Yes[3]	FFPE	90	23.00%						-	-	-			
PTCL-NOS33*	PTCL-NC	OncoScan	No	DASL Illumina	PTCL_NOS_030	Yes[4]	FFPE		35.00%	+	-	-	-	-	-	-				-
PTCL-NOS34	PTCL-NC	Agilent SurePrint	Yes[1]	HG-U133 Plus2	Yes[1]	Yes[1]	Fresh Frozen		40.00%	Reviewed in Dobay et al, Haematologica 2017										
PTCL-NOS35	PTCL-NC	Agilent SurePrint	Yes[1]	HG-U133 Plus2	Yes[1]	Yes[1]	Fresh Frozen		20.00%	Reviewed in Dobay et al, Haematologica 2017										
PTCL-NOS36*	PTCL-NC	OncoScan	No	HG-U133 Plus2	GSM472042	Yes[2]	Fresh Frozen	7.5	22.00%	+	+	-	-	-						
PTCL-NOS37*	PTCL-NC	OncoScan	No	HG-U133 Plus2	GSM1411361	Yes[3]	Fresh Frozen	80	22.00%	+	+	-	-		-	-	Partial			
PTCL-NOS38	PTCL-TBX21	OncoScan	No	DASL Illumina	PTCL_NOS_032	Yes[4]	FFPE		17.00%	+	+	-	-	-	-/+	-/+				-/+
PTCL-NOS39*	PTCL-TBX21	OncoScan	No	DASL Illumina	PTCL_NOS_070	Yes[4]	FFPE		29.00%	+		-	-/+	-	-	Rare+				-
PTCL-NOS40*	PTCL-TBX21	OncoScan	No	DASL Illumina	PTCL_NOS_015	Yes[4]	FFPE		27.00%	+	-	-	+	-	-	-				-

PTCL-NOS41*	PTCL-TBX21	OncoScan	No	DASL Illumina	PTCL_NOS_007	Yes[4]	FFPE		33.00%	+	+	-	-	-	-	-					-
PTCL-NOS42	PTCL-TBX21	OncoScan	No	DASL Illumina	PTCL_NOS_012	Yes[4]	FFPE		25.00%	+	-	-	-	-	-	-					-
PTCL-NOS43	PTCL-TBX21	OncoScan	No	DASL Illumina	PTCL_NOS_018	Yes[4]	FFPE		22.00%	+	+	-	-	-	-	-					-
PTCL-NOS44*	PTCL-TBX21	OncoScan	No	DASL Illumina	PTCL_NOS_062	Yes[4]	FFPE		25.00%	+	+	-	Rare+	-	+	-					-
PTCL-NOS45	PTCL-TBX21	Agilent SurePrint	Yes[1]	HG-U133 Plus2	Yes[1]	Yes[1]	Fresh Frozen		25.00%	Reviewed in Dobay et al, Haematologica 2017											
PTCL-NOS46	PTCL-TBX21	Agilent SurePrint	Yes[1]	HG-U133 Plus2	Yes[1]	Yes[1]	Fresh Frozen		21.00%	Reviewed in Dobay et al, Haematologica 2017											
PTCL-NOS47	PTCL-TBX21	Agilent SurePrint	Yes[1]	HG-U133 Plus2	Yes[1]	Yes[1]	Fresh Frozen		24.00%	Reviewed in Dobay et al, Haematologica 2017											
PTCL-NOS48	PTCL-TBX21	Agilent SurePrint	Yes[1]	HG-U133 Plus2	Yes[1]	Yes[1]	Fresh Frozen		23.00%	Reviewed in Dobay et al, Haematologica 2017											
PTCL-NOS49	PTCL-TBX21	Agilent SurePrint	Yes[1]	HG-U133 Plus2	Yes[1]	Yes[1]	Fresh Frozen		21.00%	Reviewed in Dobay et al, Haematologica 2017											
PTCL-NOS50	PTCL-TBX21	Agilent SurePrint	Yes[1]	HG-U133 Plus2	Yes[1]	Yes[1]	Fresh Frozen		22.00%	Reviewed in Dobay et al, Haematologica 2017											
PTCL-NOS51	PTCL-TBX21	Agilent SurePrint	Yes[1]	HG-U133 Plus2	Yes[1]	Yes[1]	Fresh Frozen		28.00%	Reviewed in Dobay et al, Haematologica 2017											
PTCL-NOS52	PTCL-TBX21	Agilent SurePrint	Yes[1]	HG-U133 Plus2	Yes[1]	Yes[1]	Fresh Frozen		18.00%	Reviewed in Dobay et al, Haematologica 2017											
PTCL-NOS53	PTCL-TBX21	Agilent SurePrint	Yes[1]	HG-U133 Plus2	Yes[1]	Yes[1]	Fresh Frozen		46.00%	Reviewed in Dobay et al, Haematologica 2017											
PTCL-NOS54	PTCL-TBX21	Agilent SurePrint	Yes[1]	HG-U133 Plus2	Yes[1]	Yes[1]	Fresh Frozen		49.00%	Reviewed in Dobay et al, Haematologica 2017											
PTCL-NOS55	PTCL-TBX21	Agilent SurePrint	Yes[1]	HG-U133 Plus2	Yes[1]	Yes[1]	Fresh Frozen		30.00%	Reviewed in Dobay et al, Haematologica 2017											
PTCL-NOS56	PTCL-TBX21	Agilent SurePrint	Yes[1]	HG-U133 Plus2	Yes[1]	Yes[1]	Fresh Frozen		27.00%	Reviewed in Dobay et al, Haematologica 2017											
PTCL-NOS57	PTCL-TBX21	Agilent SurePrint	Yes[1]	HG-U133 Plus2	Yes[1]	Yes[1]	Fresh Frozen		27.00%	Reviewed in Dobay et al, Haematologica 2017											
PTCL-NOS58	PTCL-TBX21	Agilent SurePrint	Yes[1]	HG-U133 Plus2	Yes[1]	Yes[1]	Fresh Frozen		26.00%	Reviewed in Dobay et al, Haematologica 2017											
PTCL-NOS59	PTCL-TBX21	OncoScan	No	HG-U133 Plus2	GSM1411403	Yes[3]	FFPE		22.00%						-	-	-				
PTCL-NOS60*	PTCL-TBX21	OncoScan	No	HG-U133 Plus2	GSM1411440	Yes[3]	FFPE	60	60.00%						-	-	+				
PTCL-NOS61*	PTCL-TBX21	OncoScan	No	HG-U133 Plus2	GSM1411371	Yes[3]	Fresh Frozen	30	30.00%	+	+	-	+	-	-	-	-				
PTCL-NOS62	PTCL-TBX21	OncoScan	No	HG-U133 Plus2	GSM1411439	Yes[3]	Fresh Frozen	60	23.00%	+	-	-	Partial	Partial	-	Partial	Partial				
PTCL-NOS63	PTCL-TBX21	OncoScan	No	HG-U133 Plus2	GSM1411448	Yes[3]	Fresh Frozen		21.00%	+	+	-	+	Partial							
PTCL-NOS64*	PTCL-TBX21	OncoScan	No	HG-U133 Plus2	Pending GEO Deposit	No	Fresh Frozen		22.00%												
PTCL-NOS65	PTCL-TBX21	OncoScan	No	HG-U133 Plus2	GSM1411422	Yes[3]	FFPE	60	30.00%						-	-	-				
PTCL-NOS66*	PTCL-TBX21	SNP 250K	No	HG-U133 Plus2	GSM1411349	Yes[3]	Fresh Frozen	60	25.00%	+	+	-	-	-	-	-	-				-
PTCL-NOS67*	PTCL-TBX21	SNP 250K	No	HG-U133 Plus2	GSM1411346	Yes[3]	Fresh Frozen	60	24.00%	+	+	+	-		-	-	-				
PTCL-NOS68*	PTCL-TBX21	Not Available	No	HG-U133 Plus2	GSM1411388	Yes[3]	FFPE		Not Available	+	+		-		-	Partial					
PTCL-NOS69*	PTCL-TBX21	Not Available	No	HG-U133 Plus2	GSM1411398	Yes[3]	FFPE		Not Available	+	+		-		-	-					
PTCL-TFH1*	PTCL-TFH	OncoScan	No	DASL Illumina	PTCL_NOS_066	Yes[4]	FFPE		20.00%	+	-	-	-	-	+	+					+
PTCL-TFH2*	PTCL-TFH	OncoScan	No	DASL Illumina	PTCL_NOS_067	Yes[4]	FFPE		28.00%	+	-	+		-	+	-					+
PTCL-TFH3	PTCL-TFH	OncoScan	No	HG-U133 Plus2	GSM1411329	Yes[3]	Fresh Frozen	40	16.00%	+	+	-	+	+	+	+	+				
PTCL-TFH4	PTCL-TFH	OncoScan	No	HG-U133 Plus2	GSM1411450	Yes[3]	FFPE	60	32.00%						-	+	+				
PTCL-TFH5	PTCL-TFH	OncoScan	No	HG-U133 Plus2	GSM1411452	Yes[3]	Fresh Frozen	60	20.00%	+			-	+	+	+	+				
PTCL-TFH6	PTCL-TFH	OncoScan	No	HG-U133 Plus2	GSM1411336	Yes[3]	Fresh Frozen	60	22.00%						+	+	+				
PTCL-TFH7	PTCL-TFH	OncoScan	No	HG-U133 Plus2	GSM1411465	Yes[3]	Fresh Frozen	60	24.00%	+	-	-		Partial	+	+	+				Partial
PTCL-TFH8*	PTCL-TFH (Expression)	OncoScan	No	HG-U133 Plus2	GSM1411302	Yes[3]	FFPE	30	32.00%						-	Partial	Partial				
PTCL-TFH9	PTCL-TFH (Expression)	OncoScan	No	HG-U133 Plus2	GSM1411411	Yes[3]	FFPE	80	19.00%						-	Partial	Partial				
PTCL-TFH10	PTCL-TFH (Expression)	OncoScan	No	HG-U133 Plus2	GSM1411451	Yes[3]	Fresh Frozen		24.00%	+	+	-	Weak	-		Weak					
PTCL-TFH11	PTCL-TFH (Expression)	OncoScan	No	HG-U133 Plus2	GSM472092	Yes[2]	FFPE		29.00%						-	-	Partial				
PTCL-TFH12	PTCL-TFH (Expression)	OncoScan	No	HG-U133 Plus2	GSM1411458	Yes[3]	Fresh Frozen		20.00%	+	+	-									
PTCL-TFH13*	PTCL-TFH	SNP 250K	No	HG-U133 Plus2	GSM1411353	Yes[3]	Fresh Frozen	80	33.00%	+	+	-		-	+	Partial	Partial				
PTCL-TFH14*	PTCL-TFH	SNP 250K	No	HG-U133 Plus2	GSM1411363	Yes[3]	Fresh Frozen	80	22.00%	+	+	-		+	+	-	+				+
PTCL-TFH15	PTCL-TFH (Expression)	SNP 250K	No	HG-U133 Plus2	GSM472082	Yes[2]	Fresh Frozen	37.5	45.00%	+	|	-									

1. Dobay MP, Lemonnier F, Missiaglia E, Bastard C, Vallois D, Jais JP, et al. Integrative clinicopathological and molecular analyses of angioimmunoblastic T-cell lymphoma and other nodal lymphomas of follicular helper T-cell origin. Haematologica. 2017;102(4):e148-e151.

2. Iqbal J, Weisenburger DD, Greiner TC, Vose JM, McKeithan T, Kucuk C, et al. Molecular signatures to improve diagnosis in peripheral T-cell lymphoma and prognostication in angioimmunoblastic T-cell lymphoma. Blood. 2010;115(5):1026-1036.

3. Iqbal J, Wright G, Wang C, Rosenwald A, Gascoyne RD, Weisenburger DD, et al. Gene expression signatures delineate biological and prognostic subgroups in peripheral T-cell lymphoma. Blood. 2014;123(19):2915-2923.

4. Piccaluga PP, Fuligni F, De Leo A, Bertuzzi C, Rossi M, Bacci F, et al. Molecular profiling improves classification and prognostication of nodal peripheral T-cell lymphomas: results of a phase III diagnostic accuracy study. Journal of clinical oncology : official journal of the American Society of Clinical Oncology. 2013;31(24):3019-3025.

Table S2: Genomic characterstics and primers used to evaluate four T-cell lymphoma cell lines.

TP53 and PTEN DNA CN status in 4 T-cell lymphoma cell lines normalized to the RPL13A housekeeping gene compared to tonsil.

Cell Line	TP53 DNA CN	PTEN DNA CN
Jurkat	2N	2N
T8ML1	2N	Gain
MAC-1	2N	2N
HuT78	Single Loss	2N

Mutation status of 4 T-cell lymphoma cells lines as collected from literature.

Cell Line	TP53 Mutation Status	PTEN Mutation Status
Jurkat	Nonsense, Splicing	Frameshift Insertion; Missense
T8ML1	Not Available	Not Available
MAC-1	No Evidence	No Evidence
HuT78	Nonsense	None Reported

Primer sequences used to determine DNA CN status of PTEN and TP53.

Gene	Direction	Sequence
PTEN	Forward	5'-CCACAAAGTGCCTCGTTTAC-3'
PTEN	Reverse	5'-GAAGGCAACTCTGCCAAATAC-3'
TP53	Forward	5'-TGCTGCAAGAGGCAGAAA-3'
TP53	Reverse	5'-GTCAGTCGTGGAAGTGAGAAG-3'

Table S3: Basic clinical characteristics of molecularly classified PTCL cases.

				PTCL-NOS Molecular Subgroups			
		AITL	PTCL-NOS	GATA3+	TBX21+	Unclassifiable	PTCL-TFH
	Count in Study	**35**	**67**	**32**	**30**	**5**	**15**
Age at Diagnosis (Years)	**Median**	67	65	68	65	58	61
	Range	45-87	15-97	19-97	15-81	40-81	28-76
	<60	5	22	9	10	2	7
	≥60	30	38	21	15	3	7
Gender	**Male**	18	42	24	13	5	9
	Female	17	18	6	12	0	5

Table S4: DAVID analysis of genes that were gained or amplified in AITL with concordant significantly increased mRNA expression.

Category	Term	Count	%	PValue	Genes	List Total	FDR
BIOCARTA	h_ptc1Pathway:Sonic Hedgehog (SHH) Receptor Ptc1 Regulates cell cycle	4	0.672268908	0.004493931	CCNB1, CCNH, CDK7, CDC25C	54	4.919954082
KEGG_PATHWAY	hsa03015:mRNA surveillance pathway	8	1.344537815	0.0184916	SYMPK, PPP2CA, PPP2CB, PPP2R5C, CPSF7, ETF1, PPP2R2B, DAZAP1	207	21.37137795
KEGG_PATHWAY	hsa04071:Sphingolipid signaling pathway	9	1.512605042	0.026527021	S1PR2, SGPL1, PPP2CA, PPP2CB, PPP2R5C, SMPD1, MAPK9, NSMAF, PPP2R2B	207	29.27202582
KEGG_PATHWAY	hsa03018:RNA degradation	7	1.176470588	0.02679344	CNOT8, EXOSC4, BTG3, LSM7, EXOSC5, SKIV2L2, EXOSC1	207	29.52097072
KEGG_PATHWAY	hsa04922:Glucagon signaling pathway	8	1.344537815	0.0279187	ATF4, PRMT1, ADCY2, PYGM, PGAM1, PDE3B, CREB3L1, SIK1	207	30.56353346
KEGG_PATHWAY	hsa04110:Cell cycle	9	1.512605042	0.031456908	CDKN1C, CCNB1, CCND1, CCNH, PTTG1, CDK7, SKP1, CDC25C, BUB3	207	33.74974927
KEGG_PATHWAY	hsa04114:Oocyte meiosis	8	1.344537815	0.043714683	PGR, ADCY2, PPP2CA, PPP2CB, PPP2R5C, PTTG1, SKP1, CDC25C	207	43.77460138
KEGG_PATHWAY	hsa03008:Ribosome biogenesis in eukaryotes	7	1.176470588	0.044828056	GTPBP4, REXO2, SNU13, RPP30, NHP2, AK6, RIOK2	207	44.61205261
BIOCARTA	h_cellcyclePathway:Cyclins and Cell Cycle Regulation	4	0.672268908	0.045404609	CCNB1, CCND1, CCNH, CDK7	54	40.57742543
BIOCARTA	h_btg2Pathway:BTG family proteins and cell cycle regulation	3	0.504201681	0.047556018	PRMT1, CCND1, CHAF1B	54	42.06040362
BIOCARTA	H_gsk3Pathway:Inactivation of Gsk3 by AKT causes accumulation of b-catenin in Alveolar Macrophages	4	0.672268908	0.055175082	IRAK1, CCND1, TOLLIP, PPP2CA	54	47.04531683

*Only showing results with a false discovery rate (FDR) ≤50%.

Table S5: DAVID analysis of genes located on chromosome 5 that were significantly highly expressed in AITL cases with a chromosome 5 gain.

Category	Term	Count	%	PValue	Genes	List Total	FDR
BIOCARTA	h_ptc1Pathway:Sonic Hedgehog (SHH) Receptor Ptc1 Regulates cell cycle	4	4.210526316	4.91813E-05	CCNB1, CCNH, CDK7, CDC25C	13	0.046703684
KEGG_PATHWAY	hsa04110:Cell cycle	5	5.263157895	0.003732756	CCNB1, CCNH, PTTG1, CDK7, CDC25C	37	4.214429167
KEGG_PATHWAY	hsa04914:Progesterone-mediated oocyte maturation	4	4.210526316	0.010201251	CCNB1, ADCY2, MAPK9, CDC25C	37	11.13546085
BIOCARTA	h_cellcyclePathway:Cyclins and Cell Cycle Regulation	3	3.157894737	0.013651153	CCNB1, CCNH, CDK7	13	12.2391434
KEGG_PATHWAY	hsa04114:Oocyte meiosis	4	4.210526316	0.018689714	ADCY2, PPP2CA, PTTG1, CDC25C	37	19.5249884
BBID	80.T_cell_Activation	3	3.157894737	0.035397661	IL4, MAPK9, IL13	6	23.9890314

*Only showing results with a false discovery rate (FDR) ≤30%.

Table S6: DAVID analysis of genes that were significantly highly expressed in AITL cases without a chromosome 5 gain.

Category	Term	Count	%	PValue	Genes	List Total	FDR
KEGG_PATHWAY	hsa05202:Transcriptional misregulation in cancer	20	2.400960384	5.38E-05	CCNT2, ASPSCR1, PLAT, ERG, FLT3, RXRA, RELA, TGFBR2, IGF1, TSPAN7, MAX, CDKN1B, FLI1, ID2, ITGB7, ETV6, PBX3, RUNX2, CD14, KLF3	285	0.069303339
BIOCARTA	h_nthiPathway:NFkB activation by Nontypeable Hemophilus influenzae	7	0.840336134	0.002673019	MYD88, TGFBR1, RELA, CREBBP, TGFBR2, IL1B, IKBKB	102	3.277490148
KEGG_PATHWAY	hsa04060:Cytokine-cytokine receptor interaction	20	2.400960384	0.00282763	FLT3, TGFBR1, TGFBR2, KITLG, CXCR2, CXCL12, IL11RA, KDR, FLT3LG, IL12RB2, ACVR2B, TNFSF10, TNFRSF11A, TNFSF11, CLCF1, IL10RA, CX3CR1, IL1B, XCR1, GHR	285	3.584272546
KEGG_PATHWAY	hsa04514:Cell adhesion molecules (CAMs)	14	1.680672269	0.005443709	NRXN2, CLDN5, CLDN11, HLA-B, HLA-E, ITGB1, NCAM1, SIGLEC1, ITGA6, ITGA8, ITGB7, CNTN1, HLA-DPB1, SELPLG	285	6.794473631
KEGG_PATHWAY	hsa05134:Legionellosis	8	0.960384154	0.006212373	HSPA1L, CXCL1, MYD88, CXCL3, RELA, CXCL2, IL1B, CD14	285	7.718789281
KEGG_PATHWAY	hsa04151:PI3K-Akt signaling pathway	25	3.00120048	0.007689607	FGFR3, ITGB5, KITLG, ITGB1, ITGB7, TEK, GHR, THBS4, RBL2, RELA, RXRA, IGF1, IRS1, KDR, VWF, CCND1, CDKN1B, ITGA6, LPAR6, ITGA8, TSC2, ITGA7, RELN, THEM4, IKBKB	285	9.471459706
KEGG_PATHWAY	hsa04640:Hematopoietic cell lineage	10	1.200480192	0.007844491	CD55, ITGA6, FLT3, KITLG, IL1B, ANPEP, CD14, IL11RA, CD1D, FLT3LG	285	9.653433138
KEGG_PATHWAY	hsa04068:FoxO signaling pathway	13	1.56062425	0.008829682	CCND1, TNFSF10, S1PR1, CDKN1B, PLK3, RBL2, HOMER3, TGFBR1, CREBBP, TGFBR2, IGF1, IKBKB, IRS1	285	10.80305764
KEGG_PATHWAY	hsa04512:ECM-receptor interaction	10	1.200480192	0.00910194	VWF, ITGA6, ITGB7, ITGA8, ITGA7, ITGB5, SV2B, RELN, ITGB1, THBS4	285	11.11836811
KEGG_PATHWAY	hsa04064:NF-kappa B signaling pathway	10	1.200480192	0.00910194	TNFRSF11A, MYD88, TNFSF11, PTGS2, PLCG1, RELA, IL1B, IKBKB, CXCL12, CD14	285	11.11836811
KEGG_PATHWAY	hsa04144:Endocytosis	20	2.400960384	0.009692945	FGFR3, TGFBR1, TGFBR2, CXCR2, HLA-B, CYTH3, HLA-E, LDLRAP1, KDR, HSPA1L, RAB11FIP5, DAB2, ARRB2, WWP1, RAB5A, VPS4B, STAM, ARAP3, VPS36, EHD4	285	11.7992948
KEGG_PATHWAY	hsa05200:Pathways in cancer	27	3.241296519	0.01046425	FGFR3, PTGS2, KITLG, GLI2, CXCL12, ITGB1, FLT3LG, MAX, AGTR1, WNT10B, FLT3, RELA, TGFBR1, RXRA, CREBBP, TGFBR2, IGF1, APPL1, FZD4, FZD10, CCND1, CDKN1B, ITGA6, PLCG1, LPAR6, PTCH1, IKBKB	285	12.68071791
KEGG_PATHWAY	hsa04510:Focal adhesion	17	2.040816327	0.010575003	IGF1, ITGB5, ACTN2, CAPN2, ITGB1, KDR, VWF, CCND1, ARHGAP5, ITGA6, ITGA8, ITGB7, ITGA7, RELN, SHC1, PAK1, THBS4	285	12.80661344
KEGG_PATHWAY	hsa04614:Renin-angiotensin system	5	0.600240096	0.013334134	AGTR1, AGT, PRCP, CPA3, ANPEP	285	15.88946006
KEGG_PATHWAY	hsa04360:Axon guidance	12	1.44057623	0.015060172	ABLIM1, EPHA4, EPHB6, NRP1, UNC5B, SEMA3G, SEMA4B, ROBO2, PAK1, CXCL12, ITGB1, SLIT3	285	17.76654834
KEGG_PATHWAY	hsa04010:MAPK signaling pathway	19	2.280912365	0.017415329	FGFR3, RELA, TGFBR1, TGFBR2, HSPA1L, MAP3K6, MAX, MAP3K5, DUSP3, RASGRF2, ARRB2, NTRK2, IL1B, PAK1, IKBKB, RAPGEF2, CD14, DUSP7, DUSP6	285	20.26551362
KEGG_PATHWAY	hsa05132:Salmonella infection	9	1.080432173	0.020172309	CXCL1, RAB7B, MYD88, KLC1, CXCL3, RELA, CXCL2, IL1B, CD14	285	23.10176256
KEGG_PATHWAY	hsa04610:Complement and coagulation cascades	8	0.960384154	0.022513972	PLAT, C7, VWF, CD55, F10, F5, F8, PROS1	285	25.43734959
KEGG_PATHWAY	hsa04145:Phagosome	13	1.56062425	0.023281115	MARCO, RAB7B, RAB5A, ITGB5, VAMP3, HLA-B, HLA-DPB1, HLA-E, FCGR3B, ITGB1, CD14, THBS4, CLEC4M	285	26.18815507
BIOCARTA	h_tollPathway:Toll-Like Receptor Pathway	7	0.840336134	0.026983639	MYD88, RELA, TLR3, EIF2AK2, IKBKB, TLR7, CD14	102	28.86324654
KEGG_PATHWAY	hsa04810:Regulation of actin cytoskeleton	16	1.920768307	0.027059516	ARHGEF4, FGD1, FGFR3, SSH3, IQGAP2, ITGB5, ACTN2, ITGB1, ITGA6, ITGA8, ITGB7, ITGA7, ITGAD, PAK1, CD14, FGD3	285	29.7853792

*Only showing results with a false discovery rate (FDR) ≤30%.

Table S7: DAVID analysis of genes encompassed in AITL deletions in≥4 cases.

Category	Term	Count	%	PValue	Genes	List Total	FDR
KEGG_PATHWAY	hsa04150:mTOR signaling pathway	9	2.102803738	4.97E-05	PDPK1, AKT1S1, STK11, TSC2, RHEB, MLST8, RPTOR, AKT2, PIK3R2	161	0.061865193
KEGG_PATHWAY	hsa04152:AMPK signaling pathway	11	2.570093458	4.97E-04	PDPK1, CCND1, AKT1S1, STK11, TSC2, RHEB, PPP2R2D, RPTOR, LIPE, AKT2, PIK3R2	161	0.616785503
KEGG_PATHWAY	hsa05223:Non-small cell lung cancer	7	1.635514019	0.001750136	PDPK1, CCND1, RASSF1, ERBB2, CDK4, AKT2, PIK3R2	161	2.157245733
KEGG_PATHWAY	hsa05213:Endometrial cancer	6	1.401869159	0.006759157	PDPK1, CCND1, ERBB2, AXIN1, AKT2, PIK3R2	161	8.097153234
KEGG_PATHWAY	hsa00532:Glycosaminoglycan biosynthesis - chondroitin sulfate / dermatan sulfate	4	0.934579439	0.010398619	B3GALT6, XYLT2, CHST12, CSGALNACT2	161	12.20293884
KEGG_PATHWAY	hsa04910:Insulin signaling pathway	9	2.102803738	0.014496937	PDPK1, PRKAR1B, TSC2, RHEB, CRK, RPTOR, LIPE, AKT2, PIK3R2	161	16.62402902
KEGG_PATHWAY	hsa04919:Thyroid hormone signaling pathway	8	1.869158879	0.01628165	PDPK1, CCND1, NCOA3, TSC2, RHEB, AKT2, MED1, PIK3R2	161	18.48452256
KEGG_PATHWAY	hsa04932:Non-alcoholic fatty liver disease (NAFLD)	9	2.102803738	0.023621441	NDUFS7, SDHB, NDUFA3, UQCR11, GSK3A, COX4I1, DDIT3, AKT2, PIK3R2	161	25.74161578
KEGG_PATHWAY	hsa04151:PI3K-Akt signaling pathway	15	3.504672897	0.028552244	PHLPP1, PDGFA, STK11, CDK4, YWHAE, RPTOR, CCND1, PDPK1, PKN3, TSC2, RHEB, MLST8, PPP2R2D, AKT2, PIK3R2	161	30.27792437
KEGG_PATHWAY	hsa05231:Choline metabolism in cancer	7	1.635514019	0.029295197	PDPK1, PDGFA, TSC2, WASF2, RHEB, AKT2, PIK3R2	161	30.93890117

*Only showing results with a false discovery rate (FDR) ≤30%.

Table S8: DAVID analysis of genes encompassed in gains or deletions in at least 3 cases with concordant significant changes in mRNA expression in PTCL-GATA3.

Genes in CN gains/amplification with significantly increased mRNA expression

Category	Term	Count	%	PValue	Genes	List Total	FDR
KEGG_PATHWAY	hsa03040:Spliceosome	23	1.379724055	5.73E-04	SRSF1, DHX8, PRPF31, CRNKL1, LSM8, CCDC12, U2AF2, EFTUD2, U2SURP, SNRPD2, DDX5, SF3A2, BUD31, HNRNPM, RBM8A, ISY1, U2AF1, LSM5, SNRPE, THOC1, RBM17, DDX42, TXNL4A	541	0.753841093
KEGG_PATHWAY	hsa03460:Fanconi anemia pathway	13	0.779844031	6.27E-04	FANCL, SLX4, FAAP100, POLI, FANCD2, TELO2, RMI2, PALB2, ERCC4, UBE2T, BRCA1, ERCC1, TOP3B	541	0.825367402
KEGG_PATHWAY	hsa03010:Ribosome	23	1.379724055	7.82E-04	RPL18, MRPS17, RPL19, RPL14, RPL15, RPL27, RPS15A, MRPS5, MRPL9, RPS2, MRPL30, MRPL20, RPL29, MRPL24, MRPL10, MRPL15, MRPS9, RPL7, RPL32, RPL31, RPL8, MRPL32, RPS27A	541	1.028467351
KEGG_PATHWAY	hsa04070:Phosphatidylinositol signaling system	17	1.019796041	0.003572098	PRKCA, PIK3CG, IMPAD1, CDIPT, SYNJ1, PIP5K1C, PI4KB, MTMR3, MTMR14, DGKB, DGKE, PLCD1, INPP4A, PIP4K2A, IP6K1, PIP4K2B, IP6K2	541	4.616423374
KEGG_PATHWAY	hsa03050:Proteasome	10	0.599880024	0.006069154	PSMA2, PSMB4, PSMC5, PSMC2, PSMD2, PSMD3, PSMD4, PSME3, PSME4, PSMD6	541	7.725651335
KEGG_PATHWAY	hsa04144:Endocytosis	32	1.919616077	0.010164351	RAB7A, CLTB, CYTH1, RAB5C, CHMP4B, AP2S1, CHMP7, ASAP1, PIP5K1C, ARF5, ARFGEF2, ARFGEF1, AP2B1, WWP1, SNF8, WIPF2, VPS4B, NEDD4L, AGAP3, IL2RB, VPS45, PSD4, RAB11FIP4, ARPC1B, RAB11FIP5, RAB22A, HGS, SMURF2, PDCD6IP, VPS28, EPN1, SH3GL1	541	12.62272601
KEGG_PATHWAY	hsa01230:Biosynthesis of amino acids	13	0.779844031	0.011497155	ALDOA, BCAT2, MAT2A, ALDOB, PFKP, PGAM2, TKT, PSPH, GOT2, PKLR, MTR, RPIA, CBS	541	14.16394343
KEGG_PATHWAY	hsa05169:Epstein-Barr virus infection	25	1.49970006	0.012586442	POLR2H, PIK3CG, USP7, ITGAL, YWHAZ, CREBBP, AKAP8L, POLR3GL, POLR3C, STAT3, TRADD, HDAC5, GTF2E1, PSMC5, BCL2, SND1, PSMC2, GSK3B, PSMD2, PSMD3, PSMD4, PRKACA, PSMD6, RBPJL, MYC	541	15.40486242
KEGG_PATHWAY	hsa04932:Non-alcoholic fatty liver disease (NAFLD)	21	1.25974805	0.013359423	PIK3CG, UQCRC2, NDUFA5, NDUFB4, PPARA, NDUFA3, NDUFB10, UQCRC1, NDUFB9, NDUFAB1, NDUFA13, IL6R, COX5B, NDUFB2, NDUFA11, ATF4, GSK3B, MLX, PKLR, ERN1, UQCRB	541	16.27536359
KEGG_PATHWAY	hsa05012:Parkinson's disease	20	1.199760048	0.014144381	UQCRC2, NDUFA5, NDUFB4, NDUFA3, NDUFB10, UQCRC1, NDUFB9, ADCY5, UBE2G2, TH, NDUFAB1, NDUFA13, UBE2J2, COX5B, NDUFB2, NDUFA11, ATP5C1, PRKACA, SLC18A1, UQCRB	541	17.15087363
KEGG_PATHWAY	hsa05016:Huntington's disease	25	1.49970006	0.014203676	POLR2H, UQCRC2, NDUFB4, CLTB, UQCRC1, AP2S1, NDUFB9, NDUFAB1, COX5B, NDUFB2, AP2B1, CREB3L3, NDUFA5, NDUFA3, NDUFB10, TAF4B, CREBBP, NDUFA13, UCP1, SOD1, DNAI2, DCTN1, NDUFA11, ATP5C1, UQCRB	541	17.21666406
KEGG_PATHWAY	hsa00562:Inositol phosphate metabolism	12	0.719856029	0.020926271	PIK3CG, MTMR3, CDIPT, IMPAD1, MTMR14, SYNJ1, PIP5K1C, PLCD1, PI4KB, INPP4A, PIP4K2A, PIP4K2B	541	24.3703259
KEGG_PATHWAY	hsa00270:Cysteine and methionine metabolism	8	0.479904019	0.025782682	GOT2, MRI1, DNMT3A, MAT2A, MTR, MDH2, CBS, MPST	541	29.17779486

Genes in CN heterozygous/homozygous deletion with significantly increased mRNA expression

Category	Term	Count	%	PValue	Genes	List Total	FDR
KEGG_PATHWAY	hsa03018:RNA degradation	16	1.123595506	4.09E-04	EXOSC8, EXOSC9, SKIV2L, LSM7, CNOT2, CNOT1, PAPD5, DIS3L, CNOT7, DIS3, WDR61, DCP2, DCP1B, LSM2, XRN1, HSPA9	510	0.536963292
KEGG_PATHWAY	hsa04141:Protein processing in endoplasmic reticulum	23	1.615168539	0.006087651	P4HB, SEC24A, UBE4B, ERP29, SKP1, UBQLN1, ERLEC1, PLAA, HSPH1, BAK1, HSP90B1, SEC61B, UBE2D2, BAG1, VCP, BAG2, DNAJA1, DAD1, DNAJC5, AMFR, DNAJC3, UGGT1, EIF2AK4	510	7.719010106
KEGG_PATHWAY	hsa03013:RNA transport	23	1.615168539	0.007481857	XPOT, NCBP1, RAN, NUP88, STRAP, SNUPN, SAP18, NUP93, UBE2I, PYM1, EIF2B1, RPP14, EIF4B, PHAX, EIF4G3, SUMO1, EIF3A, NUP37, EIF3J, NUP107, NUP35, EIF2B4, NUP58	510	9.407529238
KEGG_PATHWAY	hsa04120:Ubiquitin mediated proteolysis	19	1.334269663	0.011343888	FZR1, ANAPC5, UBE3A, UBE4B, BIRC6, UBE2I, SKP1, UBE2Q2, UBE2B, UBE2N, CUL3, RNF7, UBE2D2, CUL4A, UBE2K, WWP2, KLHL9, DET1, MDM2	510	13.9369154
KEGG_PATHWAY	hsa04662:B cell receptor signaling pathway	12	0.842696629	0.011383638	KRAS, LYN, DAPP1, PIK3CB, PLCG2, PPP3CB, PPP3CC, NFKBIA, PPP3CA, CD72, BLNK, SYK	510	13.98242639
BIOCARTA	h_fasPathway:FAS signaling pathway (CD95)	8	0.561797753	0.017514835	CFLAR, PAK2, LMNB1, DFFB, CASP8, MAP2K4, LMNA, DAXX	143	19.82251104
BIOCARTA	h_ctcfPathway:CTCF: First Multivalent Nuclear Factor	7	0.491573034	0.017576458	CDKN2A, PPP2CA, TGFBR1, TGFBR3, MDM2, CTCF, PTEN	143	19.88536351
KEGG_PATHWAY	hsa04720:Long-term potentiation	11	0.77247191	0.021595028	KRAS, GRIN2B, CAMK4, PPP3CB, PPP3CC, RAP1B, PPP3CA, ITPR3, CACNA1C, PPP1CC, ITPR2	510	24.96458584
KEGG_PATHWAY	hsa05169:Epstein-Barr virus infection	23	1.615168539	0.02225396	POLR2E, LYN, RAN, POLR1D, PIK3CB, MAP2K4, NFKBIA, HLA-C, POLR2D, POLR2C, POLR3B, DDX58, CSNK2A2, GTF2E2, PSMC6, PLCG2, YWHAQ, MDM2, ENTPD1, PSMD7, TBPL1, EIF2AK4, SYK	510	25.62668771
KEGG_PATHWAY	hsa05016:Huntington's disease	23	1.615168539	0.02476604	ATP5D, CLTA, NDUFA2, POLR2E, UQCRC1, CREB3, NDUFA9, CREB1, ATP5B, CYC1, COX7A2L, VDAC2, POLR2D, POLR2C, DCTN4, NDUFA12, DCTN2, NDUFS7, GRIN2B, IFT57, CASP8, TBPL1, NDUFS1	510	28.10164842
KEGG_PATHWAY	hsa04931:Insulin resistance	15	1.053370787	0.026493382	SREBF1, CREB3, PIK3CB, CREB1, PRKAG1, NFKBIA, FOXO1, PPP1CC, PTEN, PTPN11, PPP1R3C, MGEA5, TBC1D4, PTPN1, SLC27A2	510	29.75906901

*Only showing results with a false discovery rate (FDR)≤30%.

Table S9: DAVID analysis of genes encompassed in gains or deletions in at least 3 cases with concordant significant changes in mRNA expression in PTCL-TBX21.

Genes in CN gains/amplification with significantly increased mRNA expression

Category	Term	Count	%	PValue	Genes	List Total	FDR
KEGG_PATHWAY	hsa04650:Natural killer cell mediated cytotoxicity	10	1.834862385	0.004910469	PRKCA, PIK3CG, CD244, TNF, BRAF, RAC3, CD247, PPP3R1, ZAP70, FASLG	184	6.103496152
KEGG_PATHWAY	hsa03013:RNA transport	12	2.201834862	0.005793264	NCBP2, SENP2, EIF4A3, RBM8A, NUP205, NUP210, EIF4A2, ALYREF, CYFIP2, GEMIN7, RPP40, EIF2B5	184	7.163645897
KEGG_PATHWAY	hsa03050:Proteasome	6	1.100917431	0.005799913	PSMB4, PSMD13, PSMD12, PSMB3, PSMD3, PSME4	184	7.171588758
KEGG_PATHWAY	hsa03040:Spliceosome	10	1.834862385	0.008554753	NCBP2, DHX8, EIF4A3, SRSF7, RBM8A, EFTUD2, ALYREF, U2AF1, PRPF3, SNRPG	184	10.40909776
KEGG_PATHWAY	hsa03010:Ribosome	9	1.651376147	0.027567684	MRPL24, RPL19, MRPL12, MRPL27, RPL27, MRPL9, MRPS5, MRPS21, MRPS6	184	30.0675863

Genes in CN heterozygous/homozygous deletion with significantly increased mRNA expression

Category	Term	Count	%	PValue	Genes	List Total	FDR
KEGG_PATHWAY	hsa04978:Mineral absorption	7	0.770077008	0.006704217	MT1M, MT2A, MT1E, MT1H, MT1X, MT1G, MT1F	258	8.342341982
KEGG_PATHWAY	hsa05032:Morphine addiction	9	0.99009901	0.019483923	GABRR2, OPRM1, PDE7B, GNAO1, GABRR1, GNG13, PDE10A, GRK5, CACNA1B	258	22.49289608
KEGG_PATHWAY	hsa04742:Taste transduction	6	0.660066007	0.024856764	TAS2R13, TAS2R50, TAS2R14, TAS2R19, GNG13, TAS1R1	258	27.81621456
BIOCARTA	h_deathPathway:Induction of apoptosis through DR3 and DR4/5 Death Receptors	5	0.550055006	0.029209455	TNFRSF10A, CEP104, TNFRSF10B, TNFRSF25, DFFB	60	28.46128816

*Only showing results with a false discovery rate (FDR) ≤30%.

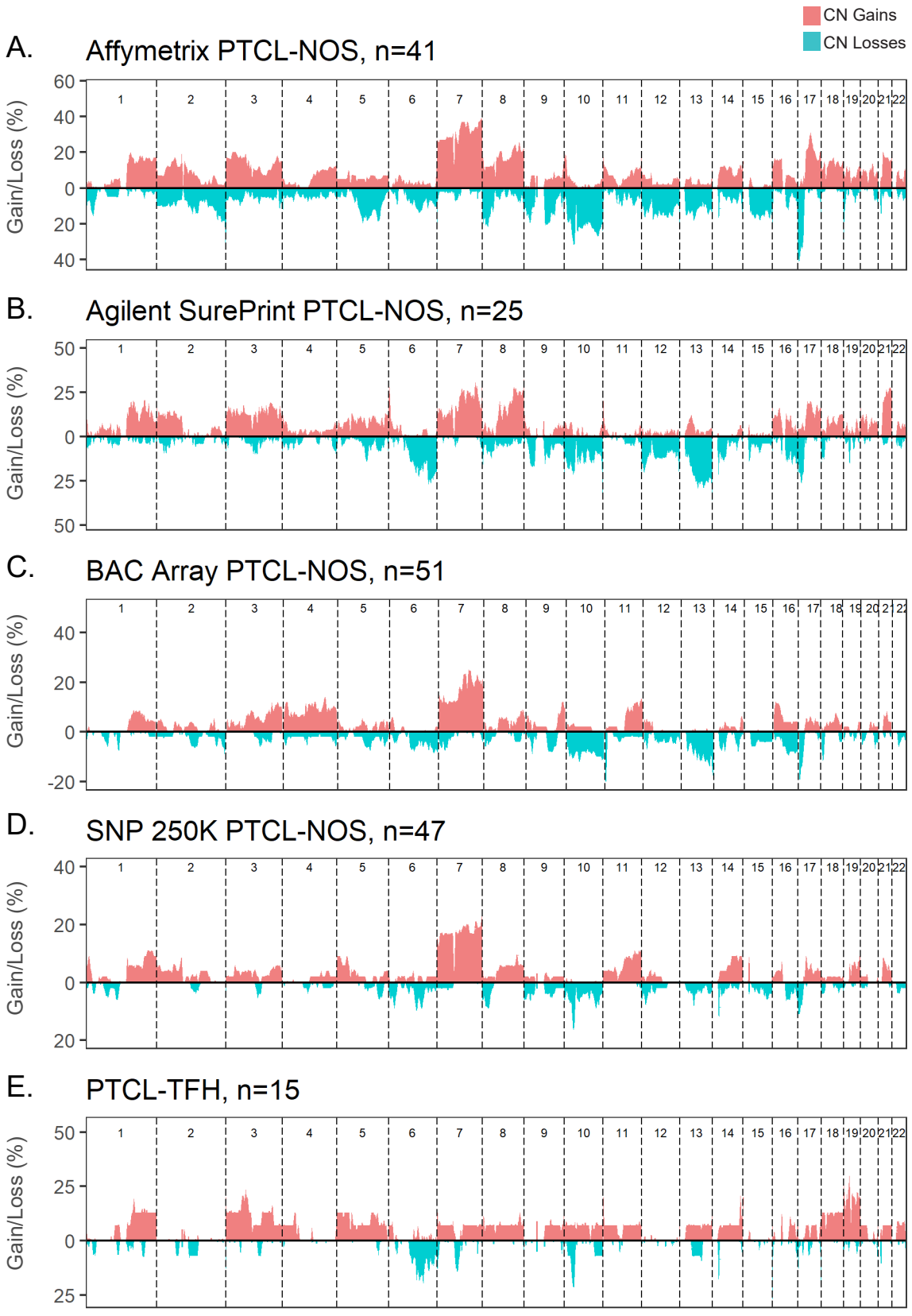

Figure S1: Frequency of chromosomal aberrations observed in four different PTCL-NOS copy number data sets or PTCL-T_{FH} cases. A. CNAs were analyzed using the OncoScan or NspI 250K platforms (Affymetrix) at UNMC. **B.** Cases from a previously published study which analyzed CNAs using the Agilent SurePrint array[1]. **C.** Cases from a previously published study which analyzed CNAs using a bacterial artificial chromosome (BAC) array[2]. **D.** Cases from a previously published study which analyzed CNAs using the Affymetrix StyI 250K platform[3]. **E.** PTCL-T_{FH} cases identified by IHC or mRNA expression analysis and excluded from the PTCL-NOS group in accordance with the WHO 2016 classification scheme.

A.

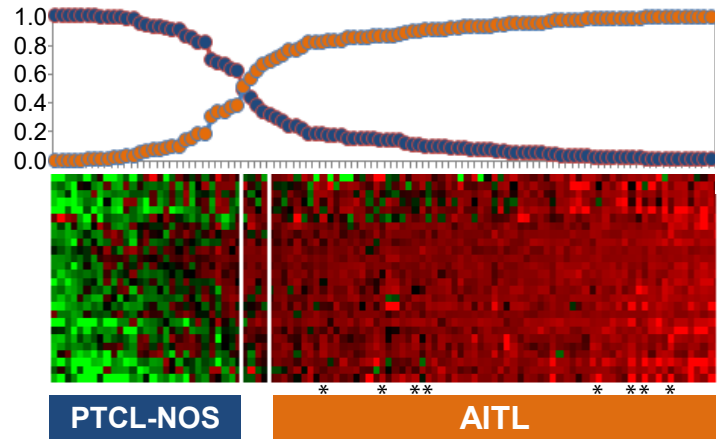

B.

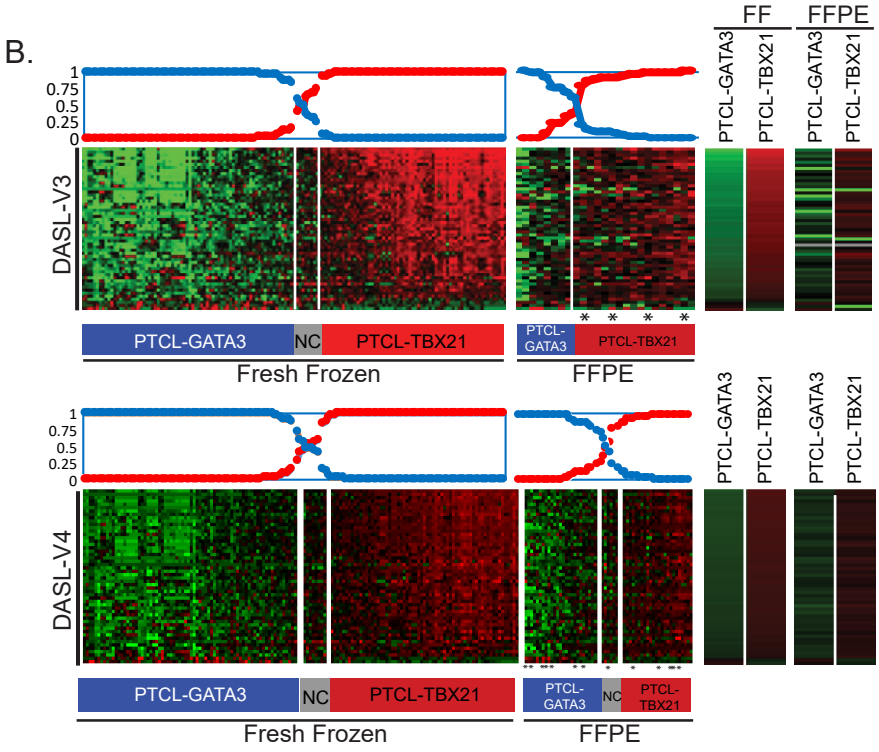

Figure S2: Classification of PTCL entities and subgroups. A. Analysis of the AITL signature genes identified on the Affymetrix HG-U133 Plus2 platform[4,5] in RNA sequencing data. The Bayesian predictor for AITL (orange) and PTCL-NOS (blue) entities are shown above the heatmap and the eight AITL cases included in the study are noted with an asterisk. **B.** PTCL-GATA3/TBX21 subgroup classification using signature genes generated from the Affymetrix HG-U133 Plus2 platform[4,5]. Robust classifier genes present in both Affymetrix and Illumina DASL V3 or DASL V4 platforms were used to molecularly classify FFPE PTCL-NOS cases[6]. The Bayesian predictor for GATA3 (blue) or TBX21 (red) subtypes are shown below the heatmaps and cases included in the study are marked with an asterisk. The Illumina HUMANREF 8_V3_0_R1_11282963_A_WGDASL (DASL V3) or Human HT 12_V4_0_R2_15002873_B_WGDASL (DASL V4) were available from a previously published dataset[6].

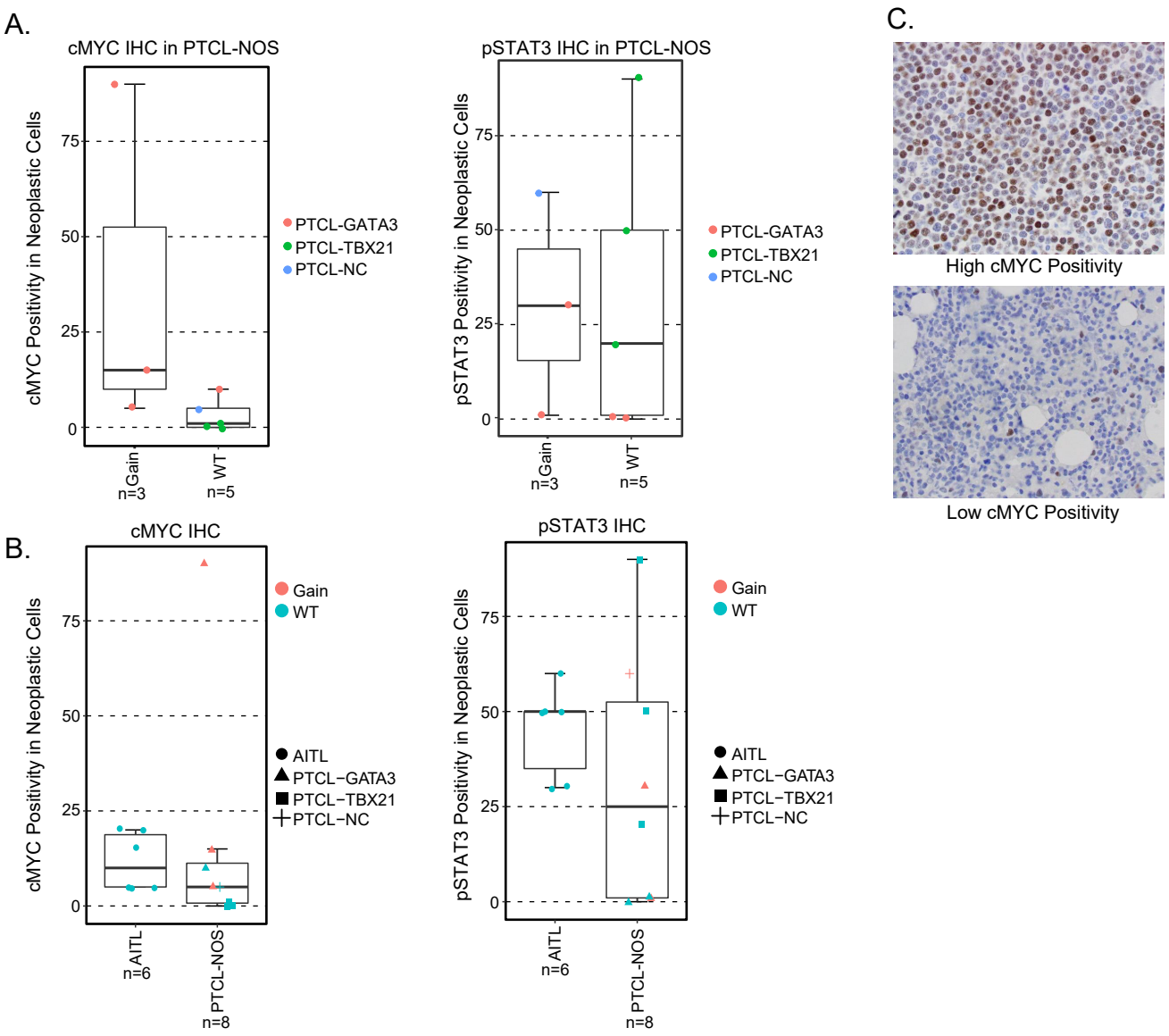

F**igure S3: Quantification of IHC staining of cMYC and pSTAT3. A.** Quantification of cMYC (left) and pSTAT3 (right) positivity in neoplastic cells by IHC in PTCL-NOS molecular subgroups delineated on the copy number state of MYC and STAT3, respectively. **B.** Quantification of cMYC (left) and pSTAT3 (right) positivity in neoplastic cells by IHC in AITL and molecular subgroups of PTCL-NOS. Colors delineate the copy number state of MYC and STAT3, respectively, and shapes depict the entity/subgroup. **C.** Representative IHC images (60x) from a highly cMYC positive and a lesser cMYC positive PTCL case.

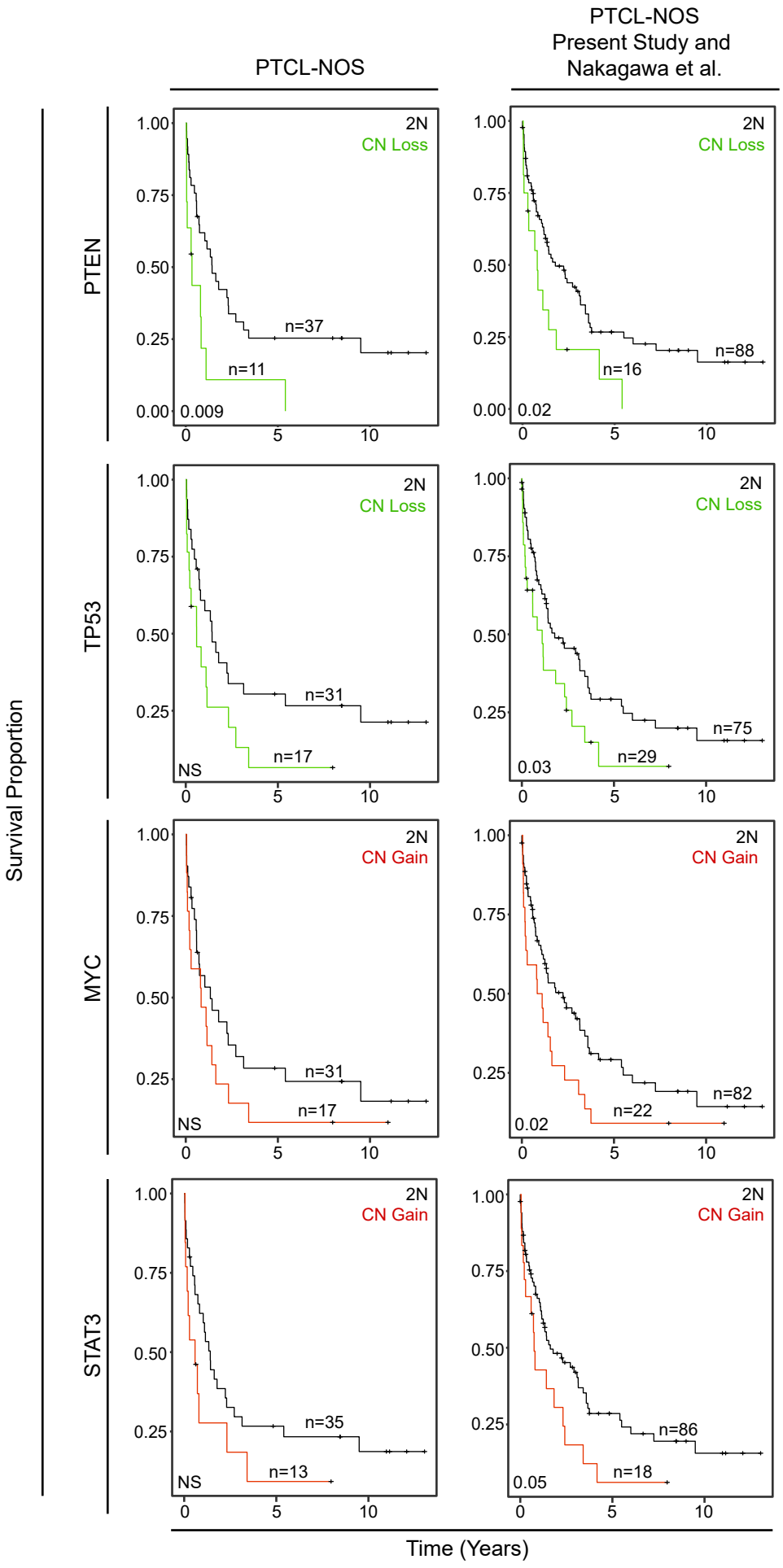

Figure S4: Overall survival associations. Kaplan-Meier curves comparing overall survival between cases with or without PTEN loss, TP53 loss, MYC gain, or STAT3 gain as indicated. The left column is comparing overall survival from the present PTCL-NOS cohort and the right column is comparing overall survival from the present PTCL-NOS cohort combined with a previously published PTCL-NOS cohort[2].

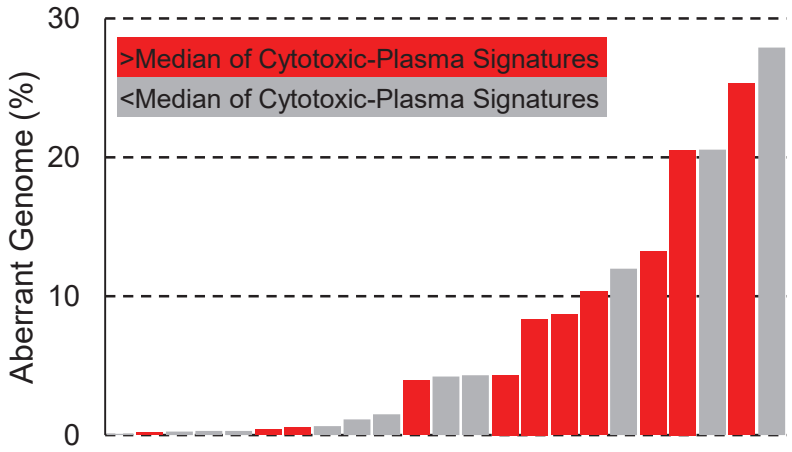

Figure S5: Percent aberrant genome distribution of PTCL-TBX21 cases with increased expression of the cytotoxic signature. The cytotoxic signature was calculated by finding the difference between the CD8+ cytotoxic and plasma cell signatures[7]. Red indicates cases with a cytotoxic signature greater than the median and gray represents cases with a cytotoxic signature lower than the median.

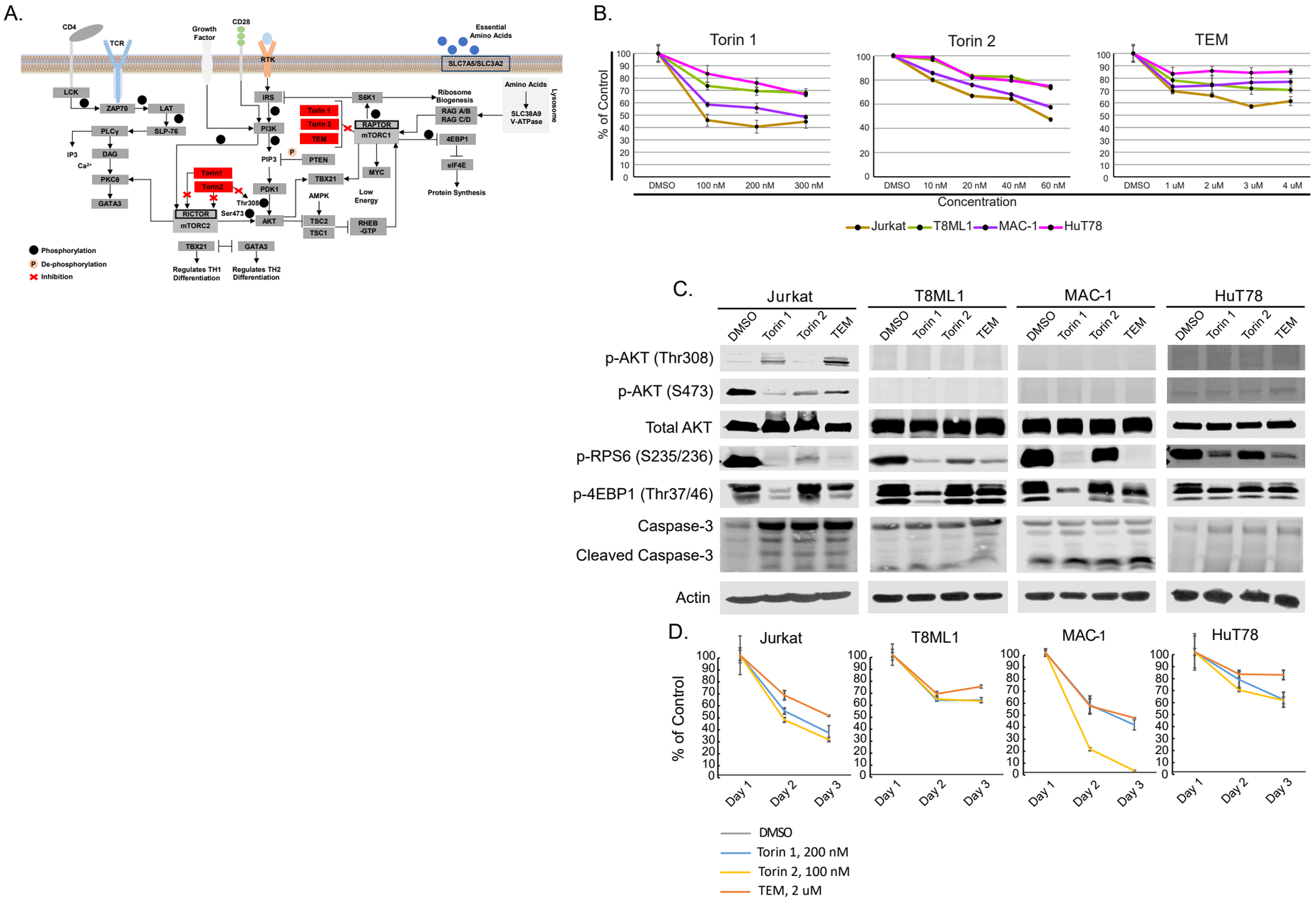

Figure S6: mTOR inhibition in T cell lines. A. mTOR schematic indicating targets of Torin 1, Torin 2, and Temsirolimus. **B.** Drug dose response curve for four T-cell lymphoma cell lines (Jurkat, T8ML1, MAC-1, and HuT78) following 24 hours of mTOR inhibitor treatment at the indicated concentrations. **C.** Western blots of Jurkat, T8ML1, MAC-1 and HuT78 cells after treatment with control (DMSO), Torin 1 (200 nM), Torin 2 (100 nM), or TEM (2 μM) for 48 hours. The inhibitors target core components of mTOR signaling and resulted in reduced phosphorylation of rapamycin-sensitive (RPS6S235) and insensitive (4EBP1T37/46) substrates of mTORC1 and mTORC2. A complex effect on AKT phosphorylation was observed in Jurkat with inhibition of AKT^{S473} phosphorylation, but increased AKT^{Thr308} phosphorylation, an effect observed with TEM and Torin1, but not with dual inhibitor Torin2. Increased cleavage of Caspase-3 upon drug treatment was prominent in Jurkat cells, indicating activation of the apoptotic pathway. **D.** PrestoBlue proliferation assay of Jurkat, T8ML1, MAC-1 and HuT78 after treatment with DMSO, Torin 1, Torin 2, or TEM at the doses depicted in the legend. Values were normalized to the control (DMSO). Jurkat cells were more sensitive to Torin1/2 compared to TEM, whereas MAC-1 was most sensitive to Torin2; T8ML1 and HuT78 were >50% viable at 48 hours. Cell lines were less sensitive to the FDA-approved mTOR inhibitor TEM, even at 2μM. Data presented represents one representative experiment of three independent experiments.

References

1. Dobay MP, Lemonnier F, Missiaglia E, Bastard C, Vallois D, Jais JP, et al. Integrative clinicopathological and molecular analyses of angioimmunoblastic T-cell lymphoma and other nodal lymphomas of follicular helper T-cell origin. Haematologica. 2017;102(4):e148-e151.
2. Nakagawa M, Nakagawa-Oshiro A, Karnan S, Tagawa H, Utsunomiya A, Nakamura S, et al. Array comparative genomic hybridization analysis of PTCL-U reveals a distinct subgroup with genetic alterations similar to lymphoma-type adult T-cell leukemia/lymphoma. Clin Cancer Res. 2009;15(1):30-38.
3. Hartmann S, Gesk S, Scholtysik R, Kreuz M, Bug S, Vater I, et al. High resolution SNP array genomic profiling of peripheral T cell lymphomas, not otherwise specified, identifies a subgroup with chromosomal aberrations affecting the REL locus. British journal of haematology. 2010;148(3):402-412.
4. Iqbal J, Weisenburger DD, Greiner TC, Vose JM, McKeithan T, Kucuk C, et al. Molecular signatures to improve diagnosis in peripheral T-cell lymphoma and prognostication in angioimmunoblastic T-cell lymphoma. Blood. 2010;115(5):1026-1036.
5. Iqbal J, Wright G, Wang C, Rosenwald A, Gascoyne RD, Weisenburger DD, et al. Gene expression signatures delineate biological and prognostic subgroups in peripheral T-cell lymphoma. Blood. 2014;123(19):2915-2923.
6. Piccaluga PP, Fuligni F, De Leo A, Bertuzzi C, Rossi M, Bacci F, et al. Molecular profiling improves classification and prognostication of nodal peripheral T-cell lymphomas: results of a phase III diagnostic accuracy study. J Clin Oncol. 2013;31(24):3019-3025.
7. Newman AM, Liu CL, Green MR, Gentles AJ, Feng W, Xu Y, et al. Robust enumeration of cell subsets from tissue expression profiles. Nat Methods. 2015;12(5):453-457.